

LETTERS

Continuously Growing Spiral Carbon Nanoparticles as the Intermediates in the Formation of Fullerenes and Nanoonions

Masaki Ozawa,^{†,‡} Hitoshi Goto,[‡] Michiko Kusunoki,[§] and Eiji Ōsawa^{*,‡,||}

Department of Integrated Biosciences, The University of Tokyo, Bunkyo-ku, Tokyo 113-8656, Japan,

Department of Knowledge-based Information Engineering, Toyohashi University of Technology,

Toyohashi, Aichi, 441-8580, Japan, Central Research Department, Fine Ceramics Center,

Mutsuno, Nagoya 456-8587, Japan, and NanoCarbon Research Institute, Chosei, Chiba 299-4395, Japan

Received: February 14, 2002; In Final Form: May 23, 2002

We report the occurrence of quasispherical Archimedean spiral carbon nanoparticles and their transformation into onion-like nested multishell fullerenes. Irradiation of electron beam onto nanosized carbon particles forms spiral nanoparticles prior to transformation into onions. In situ microscopic observation reveals that the spiral-onion conversion is reversible and progresses outward from the center of a particle. A scheme is presented whereby thermodynamically most stable onion configuration is reached through the reversible transformation with the spiral intermediate playing the role of shell-adjuster. The scheme encompasses the growth mechanism of single- as well as multishell fullerene formation.

1. Introduction

Fullerene-based carbons are clearly one of the most promising materials for nanotechnology because of the unique mechanical, electronic, magnetic, and optical properties wrapped up in great variety of structures¹. With the increasing expectation for the practical uses, elucidation of their formation mechanism becomes a critical problem for selective synthesis of each individual structure, because the yields by present methods are only about 10% for C₆₀ and much less for the higher, endohedral, and multishell fullerenes. It has been well-known that spontaneous formation of fullerenes shows distinct selectivity to give "magic numbers" for the products. For instance, fullerenes show up with discrete number of carbon atoms (ex. C₆₀, C₇₀, C₇₆, ...), and multishell fullerenes always follow

a single onion configuration (i.e. C₆₀@C₂₄₀@C₅₄₀@C₉₆₀...@C_{60n}2...^{2,3}). The mechanism of C₆₀ formation has been investigated carefully, and the ring-collapse theory⁴ involving the first occurrence of polyyne chains followed by ring formation and perfect closure of multiple-ring intermediates to cages is well accepted. On the other hand, the formation of magic configuration onions is still left unresolved, despite a few detailed studies under irradiation of electron beam.⁵⁻⁸ However, simultaneous generation of fullerenes with onions⁹ or soot particles¹⁰ indicates an underlying mechanism common for the formation of all types of fullerene networks.

We present here a new formation mechanism of multishell fullerenes based on direct and frequent observation of 3D spiral particles upon irradiation of intense electron beam onto various kinds of carbon particles and their reversible transformation into onions. This observation leads to a spiral growth hypothesis, which not only solves the long-pending riddle of the magic configuration in onion carbons but also offers a prospect for a general growth scheme of multi- and single-shell fullerenes.

* To whom correspondence should be addressed. E-mail: OsawaEiji@aol.com.

[†] The University of Tokyo.

[‡] Toyohashi University of Technology.

[§] Fine Ceramics Center.

^{||} NanoCarbon Research Institute.

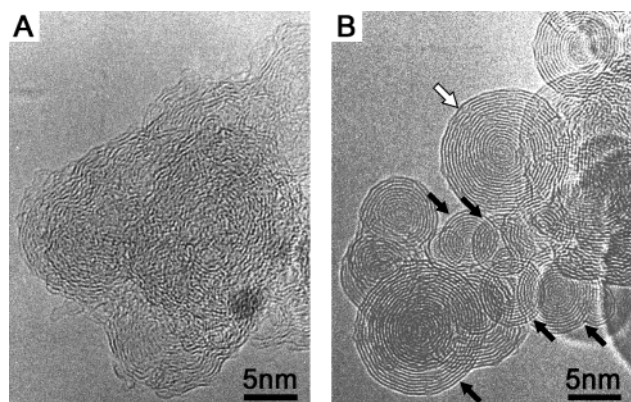


Figure 1. Conversion of commercial furnace black particles into carbon nano-onions by irradiation of focused electron beam. (A) Toka Black #8500F before irradiation. (B) The same spot with the same magnification as in A after irradiation for 20 min. A particle having a spiral core is marked with an open arrow. Five well-formed onions marked with solid arrows were analyzed for average intershell distances and shell diameters.

2. Experimental Section

Commercial furnace black having an arithmetic average diameter of 14 nm for primary particles (Toka Black #8500F, MCF grade, Tokai Carbon Co., Ltd), polyhedral carbon nanoparticles from the cathode of an arc discharge experiment, and amorphous carbons were used as starting materials. The samples dispersed in ethanol were placed onto copper grids supporting holey carbon films. Irradiation experiments were carried out at room temperature using an intense electron beam (estimated current density 150 A/cm²) in a high-resolution transmission electron microscope (HRTEM: JEOL JEM-2010) operated at 200 kV. Some images shown in this paper were captured from the video sequences of dynamic processes recorded during in situ microscopic observation. Geometry optimization of a molecular model of a double-layer nanospiroid particle was performed with MOPAC2000 version 1.33 (purchased from Fujitsu Co. under license) using MNDO Hamiltonian under UHF formalism.

3. Results and Discussion

Commercial carbon blacks^{11–14} were irradiated with a focused electron beam in a HRTEM with the anticipation that the highly defective primary particles (Figure 1A) will be changed into more ordered structures as Ugarte¹⁵ observed to occur in faceted carbon nanoparticles by the same procedure, where they are converted to thermodynamically more favorable forms. As expected, the disorder was rectified into the well-known carbon nanooxions as first observed by Ugarte¹⁵ upon bombarding polyhedral carbon nanoparticles with an electron beam, as extensive surface graphitic layers that had held the primary soot particles into small aggregates are gradually gone (Figure 1B).

To our surprise, a close look at one of the round and densely nested images in Figure 1B, marked with an open arrow, revealed it to contain a large spiral core, even though the image is considerably disturbed from place to place by dislocations. Careful repetition of irradiation experiments on various types of soot and other carbon samples, such as polyhedral carbon nanoparticles and amorphous carbons, convinced us that spiral images (Figure 2A: a remarkably clear example) almost always appear preceding the formation of concentric onion-like images with substantial lifetimes under the electron bombardment for the microscopy. Among the samples examined, we find carbon blacks are transformed most efficiently because of the hidden

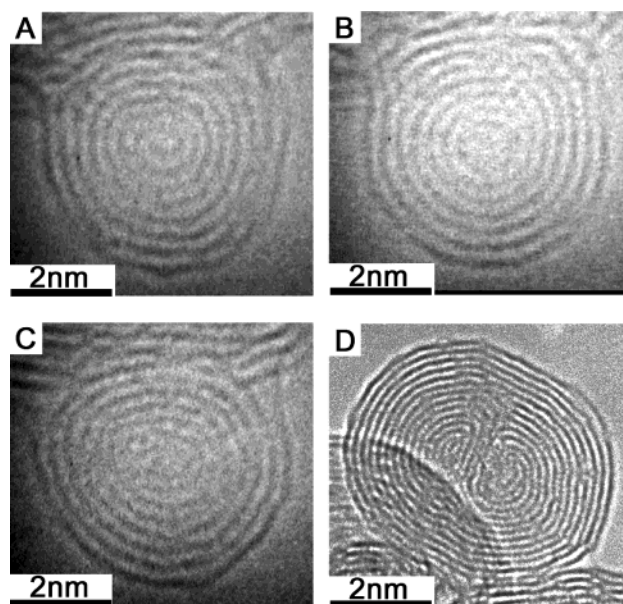


Figure 2. HRTEM micrographs of typical Archimedean spiral particles observed during bombardment of electron beam onto Toka Black #8500F. (A) A spiral image with more than seven layers. The same particle as in A (B) in an intermediate state and (C) after complete transformation into an onion. (D) An exotic particle having two spiral cores.

onion character in flaming soot as discussed later. Although irregularly shaped spirals were sometimes found at the very initial stage of spiral growth, it is difficult to prove by in situ observation with HRTEM primarily because of its size, short life, and the other carbon structures surrounding it.

In the past, spiral carbon nanoparticles have occasionally been intimated by other workers^{6,16–19} but not well examined due to ambiguous images, and the occurrence of spiral particles was considered as just an extrinsic event. On the other hand, Kroto made an important suggestion¹² that the inevitable inclusion of pentagons into flat hexagon-networks leads to curved “embryos” of soot, which grow into spiral shell particles made from continuous sheets of 5/6 networks such as an accreting snowball. Nevertheless, the 3D quasispherical spiral geometry has never been defined as far as we know. Hence, we chose a generic name “spiroid” for the structure, following the geometrical term “helicoid” for a *warped surface generated by a moving straight line which always passes through or touches a fixed helix*.²⁰ The spiroids observed throughout our work are always of the Archimedean type with equal spacing between shells, rather than the logarithmic spiral depicted by Kroto and McKay^{12,13} for their snow-accreting growth model of flaming soot particles. Exclusive formation of Archimedean spiroids indicates outstanding importance of van der Waals attraction between shells in nanostructures compared to the macroscopic world where logarithmic spirals dominate.²¹

Upon continued irradiation of the electron beam, all of the spiroid particles were found to change into onions. The transformation starts from the center of a particle and proceeds outward. Spiral images winding around the inner onion cage are sometimes visible and represent intermediate states of this process (Figure 2B). Onions thus obtained are often reconverted into spiroids by retroreactions during early stages of irradiation, whereas spiroids never appear after long irradiation (Figure 2C). Other types of spiroids such as twins (Figure 2D) and two-arm spirals also track this process. The formation of onion cages

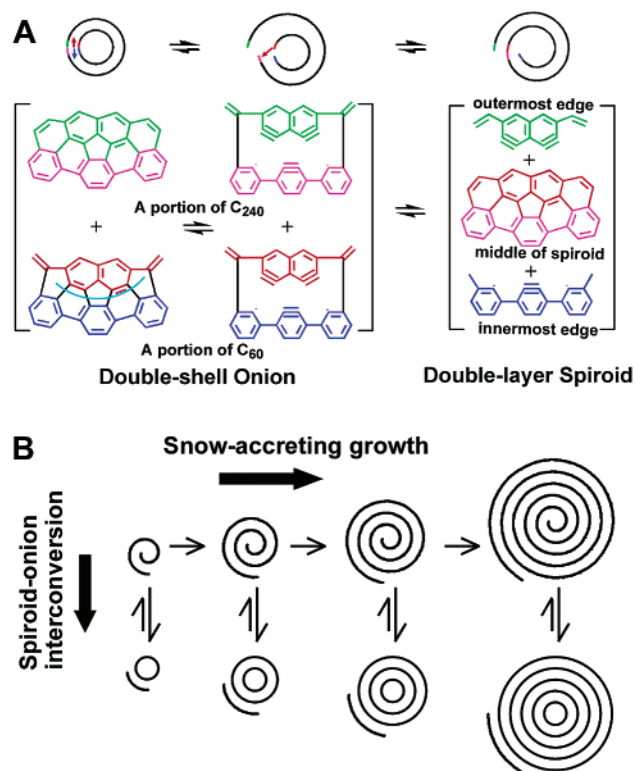


Figure 3. Proposed general formation scheme for multi- and single-shell fullerenes. (A) A hypothetical transformation of C₆₀@C₂₄₀ into a C₃₀₀ spiroid. The first step is the opening of C₆₀ by cleavage of four vicinal 5/6 bonds indicated by a light-blue curve. Formal backside substitution of reactive portion at an appropriate portion of C₂₄₀ shell regenerates a naphthalenyne-capped lip as the leaving group. Arrows in the cross-sectional view indicate the direction of reaction when the onion-to-spiroid transformation occurs. (B) Successive growth of multilayer spiroid and discrete formation of multishell fullerenes. The latter remains unchanged when the magic configuration is satisfied, otherwise the once-closed onion-like particles will revert to spiroid and then resume growing process.

has been believed to occur from outside toward inside by "internal epitaxial growth",⁵ which pertains only to graphitization.

To facilitate further discussion, we present here a molecular model of spiroid by using retroreaction, onion-to-spiroid. Let us assume that the first cleavage of skeletal bonds in one of the onion shells opens up the cage under the continuous supply of excessive energy from electron bombardment. Only the weaker 5/6 bonds will cleave (Figure 3A, left) to leave a pair of short edges containing free radical centers and/or benzyne bonds. Such an opening may involve several bonds. The innermost shell is the most strained, and hence, it is likely that the cleavage starts from the core. We further postulate the following: one of the edges thus formed (colored red in Figure 3A) attacks the shell immediately above to induce cleavage of similarly weak bonds and generates a new reactive edge, thus connecting two shells into one piece of spiral sheet as shown in the case of the simplest double-shell onion C₆₀@C₂₄₀. In larger onions, this cleavage/intershell recombination sequence will propagate radially toward the surface of the particle like a zipper action (Figure 3A).

A molecular model of a double-layer spiroid thus generated from a double-shell onion and geometry-optimized by a semiempirical MO scheme is reproduced as projections along three principal axes (Figure 4). An interesting feature of this model is that the outermost edge is lifted upward as if to expose itself for further snow-accreting growth and to protect from self-termination by reacting with its own surface. By the same token,

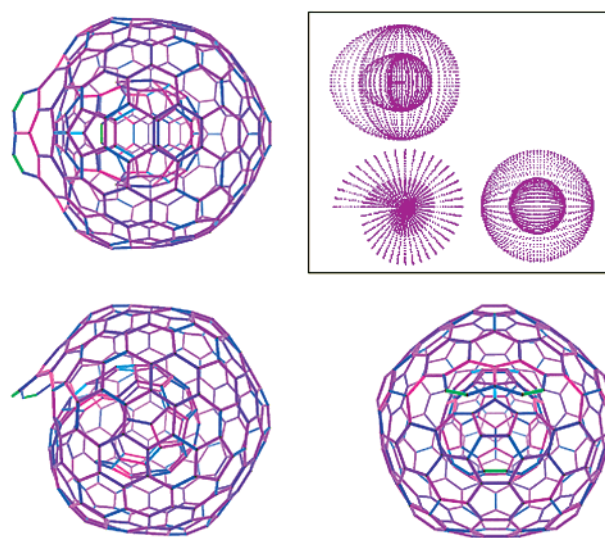


Figure 4. Molecular model of a double-layer nanospiroid particle generated by the cleavage/intershell recombination reaction as shown in Figure 3, and viewed along three principal axes. Inset shows a drawing of a corresponding numerical model reproduced by the following formulas in polar coordinates over $\theta > \pi$ and $-(\pi)/(2) \leq \phi < (\pi)/(2)$: $x = (a\theta + bx) \cos \theta \cos \phi$, $y = (a\theta + by) \sin \theta \cos \phi$, $z = (a\theta + bz) \sin \phi$, where $2\pi a$ represents the interlayer spacing, $2\pi a + bx, y, z$ correspond, respectively, to the x, y, z radii of innermost layer, and $(\theta)/(2\pi)$ is the nearest integer of $(\theta)/(2\pi)$.

the innermost edge is directed toward the inner wall of surrounding shell and seems ready to begin the reverse sequence, spiroid-to-onion. The transformation can also be reproduced by purely numerical operation (Figure 4, inset). The numerical model shown converts itself into an onion-like nested sphere simply by exchanging the coefficient of the x axis from θ to Θ . As demonstrated in the projections of models, we must be careful about the interpretation of HRTEM images, because a simple rotation of particle will make a spiroid look like an onion. In the cases of Figure 2A–C, the conclusion of spiroid–onion interconversion is safe because the particle under observation is anchored to a larger body of soot due to incomplete removal of surface graphitic layers.

Because a spiroid is clearly higher in energy than the corresponding onion, the spiroid-to-onion transformation should be an exothermic process. More difficult is the uphill retro-reaction, and in consequence, prolonged irradiation gives only onions. The only driving force of the retroreaction should be the release of large strain in the initially formed onions having highly localized pentagons and other defects. As a logical consequence of reversible reactions, formation of onion cages propagates from the center of the particles toward the surface as seen in Figure 2B, and all of the onion particles should merge into thermodynamically stable configurations after equilibration. A unique series of nested Goldberg giant fullerenes with favorable leapfrog electronic configurations in the frontier π -molecular orbitals, C₆₀@C₂₄₀@C₅₄₀@C₉₆₀...@C_{60n}..., has long been conceived^{2,3} and proposed as an ideal soot structure.^{12,13,22} As we have demonstrated,²³ only this series generates a constant intershell spacing (ca. 3.4 Å), marginally wider than the interlayer distance in graphite (3.35 Å), among all possible combinations of Goldberg fullerenes. Analyses of HRTEM micrographs support this configuration in many cases, especially for small onions or innershells of large onions.^{9,17,18,22,24} We also confirmed that the diameters of the n th shells, analyzed for n between 1 and 13, averaged over the five relatively well-formed onions in Figure 1B (indicated with solid arrows)

correlate well with those of geometry-optimized Goldberg giant fullerenes C_{60n^2} .

These observations support the downhill mechanism wherein all of the particles fall into the same energy minimum point in the course of spiroid–onion reversible conversions. It should be mentioned that the adjustments of shell sizes take place exclusively in the spiral form, whereas the disposition of pentagons in each shell is taken care of by the generalized Stone–Wales rearrangements^{25,26} that occur mainly in the onion form. The chemistry of both the reversible conversion and the Stone–Wales rearrangement is beyond the explanation of conventional organic chemistry, demonstrating the peculiar chemistry of fullerene-based networks. Discovery of spiroid intermediates thus led to the identification of a natural selection mechanism for the magic configuration in the annealing process of multishell fullerene formation. The combination of nucleation, growth, and annealing schemes presented above offers a comprehensive mechanism for the formation of fullerenes (Figure 3B).

Going back to the initially mentioned hidden onion character of the primary particles in flaming soot, we now believe they are a complex and dynamic mixture of highly defective spiroids and onions. As we demonstrated, appropriate annealing of soot should lead to onions with magic configuration. Despite several reports on the instability of onions,^{7,27} those obtained from Toka Black #8500F remain unchanged except for slight decay only on the outermost shells even after one month in air. In view of its low cost, high purity, and perfect structural homogeneity,²⁵ carbon blacks are clearly the material of choice for the production of quasi-spherical onions.

Finally, two relevant directions of research that emerge from the present work will be mentioned. First, the proposed spiral growth mechanism suggests that C_{60} and smaller members of multishell fullerenes ($n = 2-4$) will be obtained if the conventional process of carbon black manufacture is suspended at an early stage and the reaction mixture is annealed at high-temperature. Second, our mechanism may be commonly valid for the formation of multishell nanostructures, such as multiwall nanotubes²⁸ and inorganic fullerenes.²⁹

Acknowledgment. We thank Dr. X. Grabuleda for help in image analysis. The work was funded by grants from the

Ministry of Education, Science, Sports, Culture and Technology, Japan Society for Promotion of Science and Futaba Electronics Industries, Ltd. We thank Tokai Carbon Co., Ltd. for carbon black samples.

References and Notes

- (1) *Fullerenes: Chemistry, Physics, and Technology*; Kadish, K. M., Ruoff, R. S., Eds.; Wiley: New York, 2000.
- (2) Fowler, P. *Chem. Phys. Lett.* **1986**, *131*, 444–450.
- (3) Klein, D. J.; Seitz, W. A.; Schmalz, T. G. *Nature* **1986**, *323*, 703–706.
- (4) Hunter, J. M.; Fye, J. L.; Roskamp, E. J.; Jarrold, M. F. *J. Phys. Chem.* **1994**, *98*, 1810–1818.
- (5) Ugarte, D. *Carbon* **1995**, *33*, 989–993.
- (6) Qin, L.-C.; Iijima, S. *Chem. Phys. Lett.* **1996**, *262*, 252–258.
- (7) Zwanger, M. S.; Banhart, F.; Seeger, A. *J. Cryst. Growth* **1996**, *163*, 445–454.
- (8) Banhart, F. *Rep. Prog. Phys.* **1999**, *62*, 1181–1221.
- (9) Mordkovich, V. Z.; Umnov, A. G.; Inoshita, T.; Endo, M. *Carbon* **1999**, *37*, 1855–1858.
- (10) Chowdhury, K. D.; Howard, J. B.; VanderSande, J. B. *J. Mater. Res.* **1996**, *11*, 341–347.
- (11) Donnet, J.-B.; Bansal, R. C.; Wang, M.-J. *Carbon Black*; Marcel Dekker: New York, 1993.
- (12) Kroto, H. W.; McKay, K. *Nature* **1988**, *331*, 328–331.
- (13) Kroto, H. W. *Science* **1988**, *242*, 1139–1145.
- (14) Berezkin, V. I. *Phys. Solid State* **2000**, *42*, 580–585.
- (15) Ugarte, D. *Nature* **1992**, *359*, 707–709.
- (16) Kuznetsov, V. L.; Chuvilin, A. L.; Butenko, Y. V.; Mlkov, I. Y.; Titov, V. M. *Chem. Phys. Lett.* **1994**, *222*, 343–348.
- (17) Ru, Q.; Okamoto, M.; Kondo, Y.; Takayanagi, K. *Chem. Phys. Lett.* **1996**, *259*, 425–431.
- (18) Füller, T.; Banhart, F. *Chem. Phys. Lett.* **1996**, *254*, 372–378.
- (19) Donnet, J.-B. *Rubber Chem. Technol.* **1998**, *71*, 323–341.
- (20) Simpson, J. A.; Weiner, E. S. C. *The Oxford English Dictionary*, 2nd ed.; Clarendon Press: Oxford, 1989; Vol. 7, p 113.
- (21) Hargittai, I.; Hargittai, M. *Symmetry, a Unifying Concept*; Shelter: Bolinas, CA, 1994; Chapter 12.
- (22) Kroto, H. W. *Nature* **1992**, *359*, 670–671.
- (23) Yoshida, M.; Osawa, E. *Fullerene Sci. Technol.* **1993**, *1*, 55–74.
- (24) Zwanger, M. S.; Banhart, F. *Philos. Mag. B* **1995**, *72*, 149–157.
- (25) Osawa, E.; Ueno, H.; Yoshida, M.; Slanina, Z.; Zhao, X.; Nishiyama, M.; Saito, H. *J. Chem. Soc., Perkin Trans. 2* **1998**, 943–950.
- (26) Osawa, E.; Slanina, Z.; Honda, K.; Zhao, X. *Fullerene Sci. Technol.* **1998**, *6*, 259–270.
- (27) Lulli, G.; Parisini, A.; Matti, G. *Ultramicroscopy* **1995**, *60*, 187–194.
- (28) Amelinckx, S.; Bernaerts, D.; Zhang, X. B.; Van Tendeloo, G.; Van Landuyt, J. *Science* **1995**, *267*, 1334–1338.
- (29) Remskar, M.; Mrzel, A.; Skraba, Z.; Jesih, A.; Ceh, M.; Demšar, J.; Stadelmann, P.; Lévy, F.; Mihailovic, D. *Science* **2001**, *292*, 479–481.